Turkish Journal of Electrical Engineering and Computer Sciences

Volume 22 | Number 4 Article 14

1-1-2014

A low-order nonlinear amplifier model with distributed delay terms

AHMET HAYRETTİN YÜZER

ŞİMŞEK DEMİR

Turkish Journal of Electrical Engineering & Computer Sciences

http://journals.tubitak.gov.tr/elektrik/

Research Article

Turk J Elec Eng & Comp Sci
(2014) 22: 1007 – 1016

doi:10.3906/elk-1208-25

A low-order nonlinear amplifier model with distributed delay terms

Ahmet Hayrettin YÜZER[1,*], **Şimşek DEMİR**[2]
[1]Electrical and Electronics Engineering Department, Karabük University, Karabük, Turkey
[2]Electrical and Electronics Engineering Department, Middle East Technical University, Ankara, Turkey

Received: 14.08.2012 • **Accepted:** 18.01.2013 • **Published Online:** 17.06.2014 • **Printed:** 16.07.2014

Abstract: In this paper, a novel behavioral modeling technique for the characterization of memory effects of amplifiers is proposed. This characterization utilizes asymmetric intermodulation distortion (IMD) components, which are the result of a 2-tone excitation of a nonlinear amplifier. These asymmetric IMD components are represented basically by a power series, where each term in the series has its own time delay term. These time delay terms successfully justify the presence of asymmetry in the intermodulation components, which leads to the prediction of amplitude-to-amplitude and amplitude-to-phase distortions. The parameters of the model are extracted using 2-tone measurements. A 100-W peak power amplifier is examined. Model predictions are verified by the measurement results of a 4-tone stimulus. The proposed model can also be used in time domain analysis with arbitrary excitation.

Key words: Behavioral model, asymmetric IMD, AM/PM conversion, nonlinear characterization

1. Introduction

Widespread wireless applications increase the demand for high linearity and efficiency. Precise characterization of the linearity of the amplifier is critical for tuning the system accordingly, to satisfy the spectral mask as well as keeping the bit error rate and error vector magnitude (EVM) as low as possible. The spectral regrowth, adjacent channel power ratio, memory effects, asymmetry in the intermodulation distortions (IMDs), amplitude-to-amplitude (AM/AM) and amplitude-to-phase (AM/PM) distortions, gain compression, and saturation power level are some of the other performance parameters that are also measures of success of the overall system. In order to increase the success of the system in satisfying the tight spectral masks by reducing the unwanted contributions of nonlinearities, despite the decrease in efficiency, numerous amplifiers in wireless communication applications are operated in a weakly nonlinear regime [1].

On the other hand, behavioral modeling is one of the characterization techniques where only a mathematical relation between the input and output is constructed. Behavioral models can be developed in 1 of the 2 regions of modeling: baseband or passband. A baseband model suppresses the carrier frequency component and only the envelope signal is considered. In contrast, a passband model considers each cycle of the carrier frequency as well as its envelope. Although passband models can be used while designing a new amplifier, baseband models are generally used to linearize the amplifier using digital predistortion (DPD) methods.

There are a number of behavioral modeling methods published in the literature, such as the Saleh model [2], general power series expansion [3–5], memoryless polynomial modeling [6], look-up-table modeling [7,8], Volterra series [9], Wiener–Hammerstein (3-box) [10,11], Volterra [12,13], and neural networks [14]. Among these

*Correspondence: hayrettinyuzer@gmail.com

published studies [4,6–8,12–14] are baseband and [2,3,5,9,11] are passband modeling techniques. Mathematical definitions and performance comparisons of the models were also published for baseband [15–18] and passband modeling [18]. On the other hand, a new passband-type behavioral modeling is presented in the following sections of the current study.

Insight into behavioral modeling can be gained by considering the power series equation devised by Huang et al. [3] to represent only the AM/AM behavior of an amplifier:

$$V_o(t) = \sum_{k=1}^{K} a_k V_i^k(t) \tag{1}$$

Arno et al. [4] used 2 different power series equations to model both AM/AM and AM/PM distortion observed at an amplifier output. However, Ciccognani et al. [5] used 1 power series equation instead of 2, to model both AM/AM and AM/PM distortion.

The response to 2-tone excitation is a common measure for nonlinearity characterization for passband modeling techniques. A sample frequency spectrum of a 2-tone signal and the response of an amplifier to this signal are shown in Figure 1, where $\omega_{FundL} = \omega_1$, $\omega_{FundU} = \omega_2$, $\omega_{IMDL} = 2\omega_1 - \omega_2$, and $\omega_{IMDU} = 2\omega_2 - \omega_1$.

$$V_i(t) = V_1 \cos(\omega_1 t) + V_2 \cos(\omega_2 t) \tag{2}$$

$$V_0(t) = \sum_{k=1}^{K} a_k \left(V_1 \cos(\omega_1 t) + V_2 \cos(\omega_2 t)\right)^k \tag{3}$$

$$\begin{aligned} &= V_{FL} \cos(\omega_1 t) + V_{FU} \cos(\omega_2 t) + V_{IMDL} \cos((2\omega_1 - \omega_2) t) \\ &\quad + V_{IMDU} \cos((2\omega_2 - \omega_1) t) + V_{2HL} \cos(2\omega_1 t) + V_{2HU} \times \cos(2\omega_2 t) + \ldots \end{aligned} \tag{4}$$

$$V_{IMDL} = \frac{3}{4} a_3 V_1^2 V_2 + a_5 \frac{5}{4} \left[V_1^4 V_2 + \frac{3}{2} V_1^2 V_2^3\right] \tag{5}$$

$$V_{IMDU} = \frac{3}{4} a_3 V_1 V_2^2 + a_5 \frac{5}{4} \left[V_1 V_2^4 + \frac{3}{2} V_1^3 V_2^2\right] \tag{6}$$

The time domain form of this 2-tone input signal is given in Eq. (2). Considering Eq. (1) as the behavioral model and choosing K = 5, the corresponding phasor domain representation of the lower band IMD (IMDL) (IMDL – IMD at $\omega = 2\omega_1 - \omega_2$) and the upper band IMD (IMDU) (IMDU – IMD at $\omega = 2\omega_2 - \omega_1$) equations are given in Eqs. (5) and (6), respectively. Considering equal amplitude excitation, the IMD components will be of equal amplitude, $V_{IMDL} = V_{IMDU}$, which means symmetric IMD terms. However, asymmetrical distributions of the magnitude and phase of the IMD components are frequently observed in measurements, which indicate the effect of the amplifier memory. It is obvious that the asymmetric spectral distribution of the amplifier output cannot be characterized by Eq. (1).

The reason and sources of asymmetry in the magnitude and phase of the IMD components were investigated in various studies, including [19,20]. Although [2–8] did not take this memory effect into account, the other studies considered memory effects. Indeed, memoryless models are simple for modeling, but they are not precise in characterizing the amplifier due to their lack in representing asymmetry of the IMD and fundamental components. It was stated in [21] that, although memoryless predistortion demonstrated improvement for a 0.5-W handset amplifier, it was unable to give the same improvement for a 45-W power amplifier.

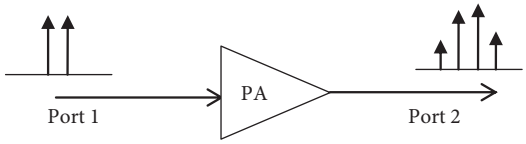

Figure 1. Two-tone excitation and response of the amplifier to that excitation.

In this paper, a new behavioral model is proposed that is capable of characterizing asymmetry in the magnitude and phase of the IMD components. The essential contribution of the proposed model is the inclusion of the time delay terms in Eq. (1). These time delay terms enhance the capability of the model for representing the consequences of the memory effects in the amplifier response.

There are various ways of modeling a physical system, by describing its local or global behavior. The most accurate mathematical model may be the one that correctly describes the physical relations in the system. When the correct representation is not used, the order of the describing function may increase very rapidly. The higher order terms indeed compensate for the missing contributions of the possibly inadequately used lower order terms. There are models presented in the literature that use several tens of terms in the power series representation. For example, Jang used a 17th-order polynomial to get an acceptable error [22].

Nonetheless, it is observed and introduced in the following sections that the proposed model in this paper can achieve acceptable accuracy with much less order of the power series. Low-order of nonlinearity not only decreases the number of unknowns, but also decreases the mathematical complexity and the computational cost considerably. As a consequence, the parametric use of a low-order model in an analytical work becomes possible.

The accuracy of the model is also related to the errors in the parameter extraction procedure. Some of the parameters might be directly correlated to a specific measurement such as linear gain. The remaining parameters are determined following a sort of curve fitting algorithm, which suffers from the local minima of the optimization processes. Functions with a low number of parameters are more immune to the local minima problem and a low number of parameters is an indication of accuracy in this sense.

2. Behavioral model having time delay terms

In this paper, a new behavioral model for nonlinear amplifiers is proposed: power series with time delay. In this model, asymmetry in the magnitude and in phase is accounted for by introducing particular time delay terms to each of the power series components in Eq. (1). The input–output relation in the proposed model is given in Eq. (7), where a_k and τ_k are real numbers. The advantage of using time delay terms and real-valued a_k instead of complex-valued a_k without time delay terms results in a different phase shift for the IMDL and IMDU, as seen in Eqs. (8) and (9), but the phase shift due to a complex-valued coefficient would be the same both for the IMDL and IMDU, as seen in Eqs. (5) and (6).

$$V_0(t) = \sum_{k=1}^{K} a_k \times V_i^k (t - \tau_k) \tag{7}$$

The smallest value of 'K', which creates asymmetry in IMD tones, is at least 2 more than the order of the IMD. For example, the asymmetries in 3rd-order IMDL and IMDU components require $K \geq 5$.

3. Measurement setup

A measurement setup, as given in Figure 2, is designed to measure both the magnitude and phase of the IMD components as well as the fundamental components. The measurement setup is presented in detail in [23]. In this measurement setup, 3 signal generators (E8257C-SGA, E8257D-SGB, and E8267D-SGC) and 1 spectrum analyzer (E4408A-SA) are used. Two of them are used for 1-tone signal generation and the other is used for the phase reference [24]. Measurement steps are given in detail in [24].

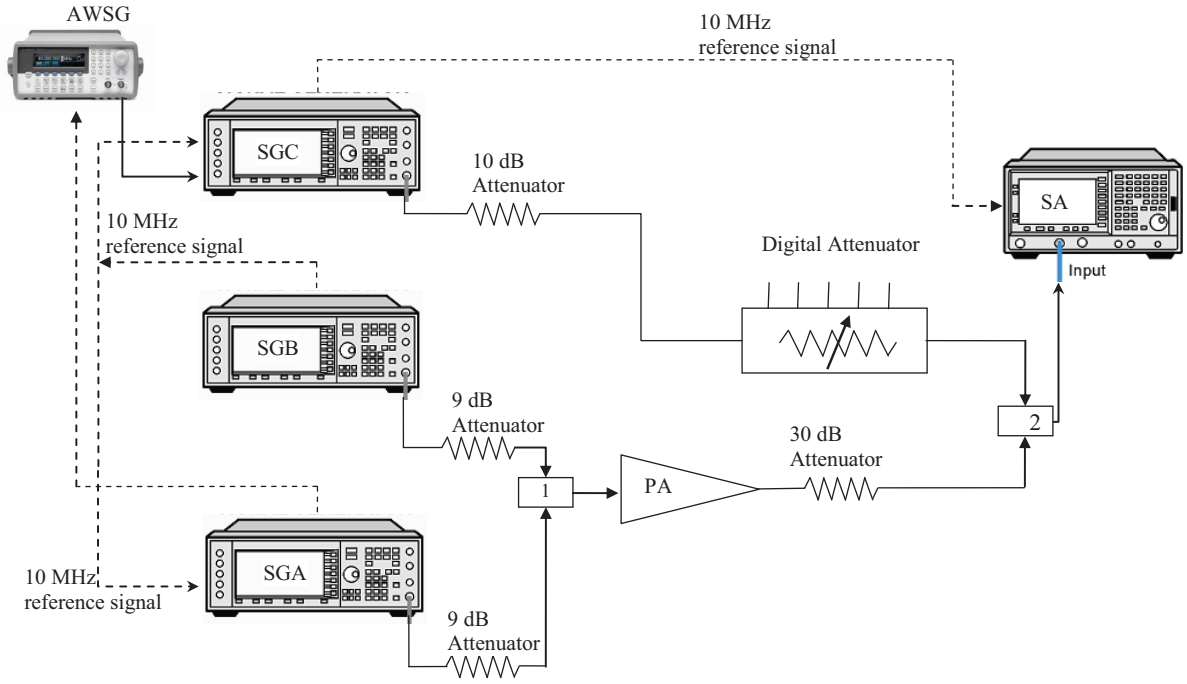

Figure 2. Schematic representation of the measurement setup.

A 100-W (50-dBm) power amplifier built for an HF communication system is examined, whose gain is 45 dB and input P_{1dB} is 6 dBm for 1-tone and 0 dBm for 2-tone excitations. P_{1dB} is –2.4 dBm for the unequal 4-tone, which is introduced in Section 5. Both the magnitude and phase of the IMD and fundamental (FUND) components are measured under 2-tone excitation, 10 MHz and 10.001 MHz, using this setup.

4. Extracting the behavioral model

As stated above, asymmetry in the magnitude and in phase of IMD can be observed if $K \geq 5$. Indeed, a higher K value may indicate a better fit of the model to the actual behavior. However, the use of high K values is not practical and this is in contradiction to our aim. Therefore, a residual error will be tolerated and the key point is the amount of that residual error. The amplifier studied in this paper is modeled with a 9th-order polynomial as given in Eq. (7). Related IMDL, IMDU, lower band fundamental (FL) and upper band fundamental (FU) components' phasor representations are given in Eqs. (8) to (11) for K = 9. The higher order terms have less contribution to the IMD signal than lower order terms when the input power is small. There is no term related to a1 in the IMDL and IMDU equation, as given in Eqs. (8) and (9). In other words, the a1 term cannot change the amplifier response at the IMD frequencies. In contrast, FL and FU are mainly affected by the a_1 term in

the linear input power region.

$$V_{IMDL}=\frac{3}{4}a_3V_1^3\angle-(2\omega_1-\omega_2)\,\tau_3 \quad +\frac{25}{8}a_5V_1^5\angle-(2\omega_1-\omega_2)\,\tau_5 \quad +\frac{735}{64}a_7V_1^7\angle-(2\omega_1-\omega_2)\,\tau_7$$

$$+\frac{1323}{32}a_9V_1^9\angle-(2\omega_1-\omega_2)\,\tau_9 \tag{8}$$

$$V_{IMDU}=\frac{3}{4}a_3V_1^3\angle-(2\omega_2-\omega_1)\,\tau_3 \quad +\frac{25}{8}a_5V_1^5\angle-(2\omega_2-\omega_1)\,\tau_5 \quad +\frac{735}{64}a_7V_1^7\angle-(2\omega_2-\omega_1)\,\tau_7$$

$$+\frac{1323}{32}a_9V_1^9\angle-(2\omega_2-\omega_1)\,\tau_9 \tag{9}$$

$$V_{FL}=a_1V_1\angle-\omega_1\tau_1 \quad +\frac{9}{4}a_3V_1^3\angle-\omega_1\tau_3 \quad +\frac{50}{8}a_5V_1^5\angle-\omega_1\tau_5$$

$$+\frac{1225}{64}a_7V_1^7\angle-\omega_1\tau_7 \quad +\frac{3969}{64}a_9V_1^9\angle-\omega_1\tau_9 \tag{10}$$

$$V_{FU}=a_1V_1\angle-\omega_2\tau_1 \quad +\frac{9}{4}a_3V_1^3\angle-\omega_2\tau_3 \quad +\frac{50}{8}a_5V_1^5\angle-\omega_2\tau_5$$

$$+\frac{1225}{64}a_7V_1^7\angle-\omega_2\tau_7 \quad +\frac{3969}{64}a_9V_1^9\angle-\omega_2\tau_9 \tag{11}$$

Extracting the behavioral model means the determination of a_k and τ_k,$k=1,3,5,7,9$. These parameters are determined by fitting Eqs. (8)–(11) to the measurement results for both the magnitude and phase (i.e. 8 different curves should be fitted using 10 parameters). The equations are not linear and the coefficients are found using MATLAB's optimization tool.

After the optimization, model predictions are checked with the measurement results of the amplifier's response to 1-tone excitation and several different unequal 4-tone excitations. Extracted model parameters of the sample amplifier are tabulated in the Table for 10-MHz and 10.001-MHz input excitations. Comparisons of the model predictions and measurement results for this 2-tone excitation are given in Figure 3, where the 'me' suffix represents the measurement results and the 'mo' suffix represents the model predictions.

Table. The extracted parameters of the 100-W amplifier for 2-tone input excitation: 10 MHz and 10.001 MHz.

a_1	a_3	a_5	a_7	a_9
161.60	53.04	81.92	20.12	–0.41
τ_1 (μ sn)	τ_3 (μ sn)	τ_5 (μ sn)	τ_7 (μ sn)	τ_9 (μ sn)
0.00	28.51	18.16	61.92	0.86

The region of interest for the optimization is the 8-dB dynamic range from –3.3 dBm to 4.7 dBm (per tone), where P_{1dB} is 0 dBm. In the optimization process, the P_{1dB} region is emphasized.

Although the error increases with a decreasing input power level, the error around the P_{1dB} point for the magnitude of the IMDL is small, and the maximum error in the magnitude of the IMDL is 4.7 dB, as seen in Figure 3a. The maximum error in the magnitude of the IMDU (Figure 3b) is 1.2 dB and the residual error in the magnitude is lower than 0.7 dB at any power level of the fundamental components (Figures 3c and 3d).

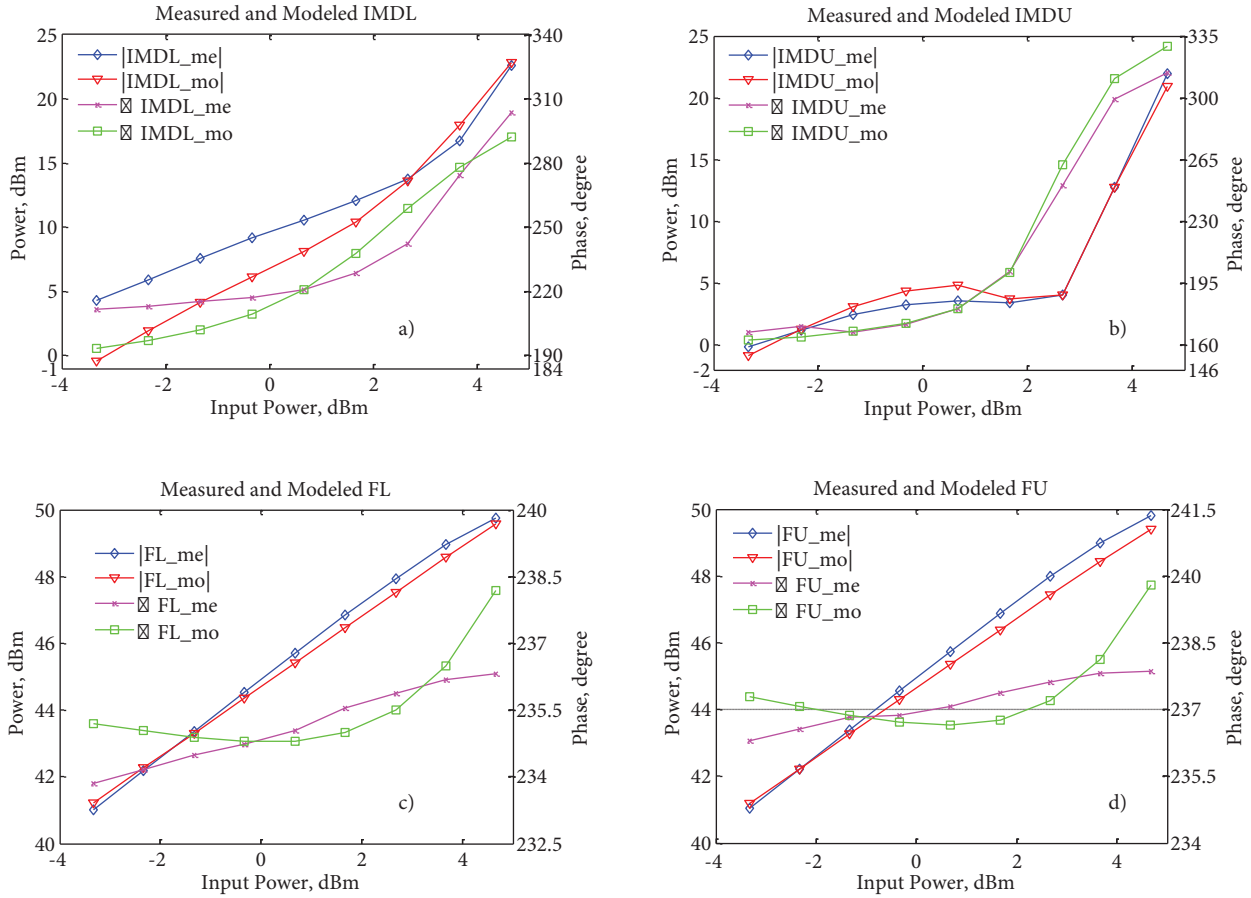

Figure 3. Comparisons of magnitudes and phases of the measurement and model outputs for 2-tone excitation; 10 MHz and 10.001 MHz: a) IMDL, b) IMDU, c) FUNDL, and d) FUNDU components.

The phase error for the fundamental components is lower than 1.9°. Although the phase error seems high with respect to the total change in the phase, this much error can be acceptable for the fundamental tone. If the polynomial order increases too much, for example, the 17th-order, as Jang [22] did, the phase error could diminish, and then the model becomes more complicated. The model phase error would increase with the decreasing order of the polynomial order. The maximum phase error is 15° for the IMDL and 18.2° for the IMDU. The estimated phase response shows similar behavior to the measured value, like that of the fundamental components.

The EVM can be used to compare measurement results and model predictions [25]. Two-tone excitation results are compared: 10 MHz and 10.001 MHz input from –3.3 dBm to 4.7 dBm power per tone. The EVM of the 2-tone model prediction for IMDL, IMDU, FL, and FU are –12.9 dB, –11.9 dB, –28.6 dB, and –25.5 dB, respectively.

The asymmetric magnitude in IMD components for high power levels can be predicted as shown in Figure 4. It should be noted that the polynomial order is limited by 9 and increasing the number of terms will decrease the residual errors. Hence, this level of error is expected. The amplifier is expected to work at around P1 dB; therefore, optimization weights are set to improve fitting around that power level.

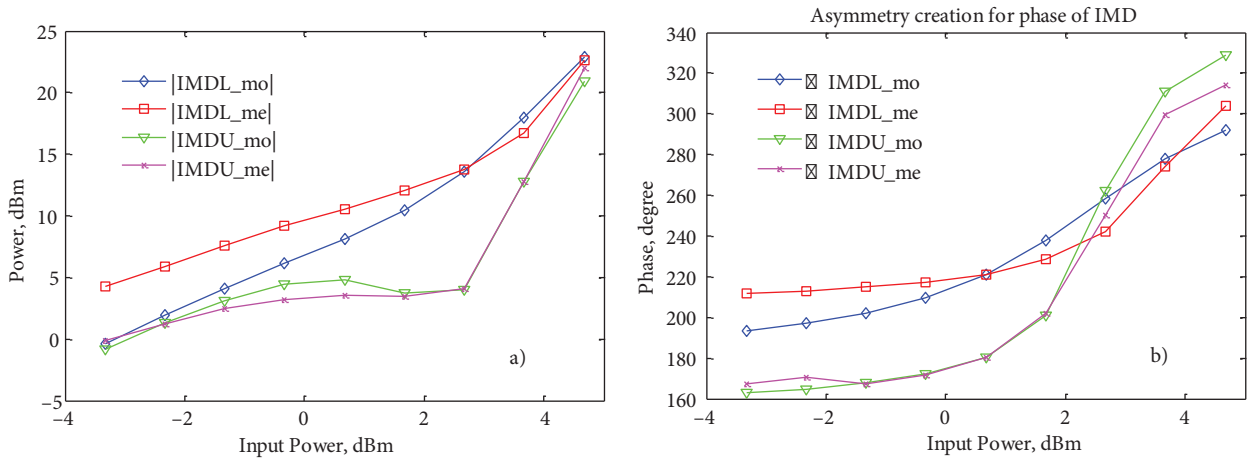

Figure 4. Modeling the asymmetry between the estimated results and measurement results w.r.t.: a) magnitudes and b) phases.

5. Unequal 4-tone comparison

The same measurement setup explained in [23] is used to measure the amplifier response to 4-tone stimuli. A mathematical representation of the input and output is given in Eqs. (12) and (13). There is a 10-dB power difference between the inner and outer tones. Measurement results and model estimations are given in Figure 5 for 4 different input power levels (from –7.8 dBm to–0.8 dBm). These values represent the power level at the input and output of the amplifier (insertion loss of the attenuator is compensated) and can be chosen higher than P1 dB.

$$V_i(t) = V_1\cos(\omega_1 t) + V_2\cos(\omega_2 t) + V_3\cos(\omega_3 t) + V_4\cos(\omega_4 t) \tag{12}$$

$$\begin{aligned} V_{0,4tone}(t) &= \sum_{k=1}^{K} a_k \left[V_1\cos(\omega_1(t-\tau_k)) + V_2\cos(\omega_2(t-\tau_k)) + V_3\cos(\omega_3(t-\tau_k)) + V_4\cos(\omega_4(t-\tau_k))\right]^k \\ &= V_{Fund1}\cos(\omega_1 t) + V_{Fund2}\cos(\omega_2 t) + V_{Fund3}\cos(\omega_3 t) \\ &\quad + V_{Fund4}\cos(\omega_4 t) + V_{IMDL1}\cos(\omega_{IMDL1} t) + V_{IMDL2}\cos(\omega_{IMDL2} t) \\ &\quad + V_{IMDU1}\cos(\omega_{IMDU1} t) + V_{IMDU2}\cos(\omega_{IMDU2} t) \end{aligned} \tag{13}$$

where ω_1, ω_2, ω_3, and ω_4 represent the frequencies of the 4 tones, namely Fund1, Fund2, Fund3, and Fund4, respectively. ω_{IMDL1} represents the lower-band first 3rd-order IMD, and, similarly, ω_{IMDL2} represents the lower-band second 3rd-order IMD. IMDL1 is affected by the interaction of the 2nd-order of Fund1 and Fund2 ($2\omega_2 - \omega_1$), the 2nd-order of Fund 2 and Fund4 ($2\omega_2 - \omega_4$), and the 3rd-order of Fund1 and Fund3 ($3\omega_1 - \omega_3$).

Although model parameters are found according to the 2-tone measurement results, model prediction errors are sufficiently small for these 4-tone excitations, as seen in Figure 5. The in-band error is lower than 1 dB. The level of the first tone in the lower adjacent channel is measured as unexpectedly smaller than that of the far-off tones, as shown in Figure 5. In contrast to this, the errors in the other tones are much smaller.

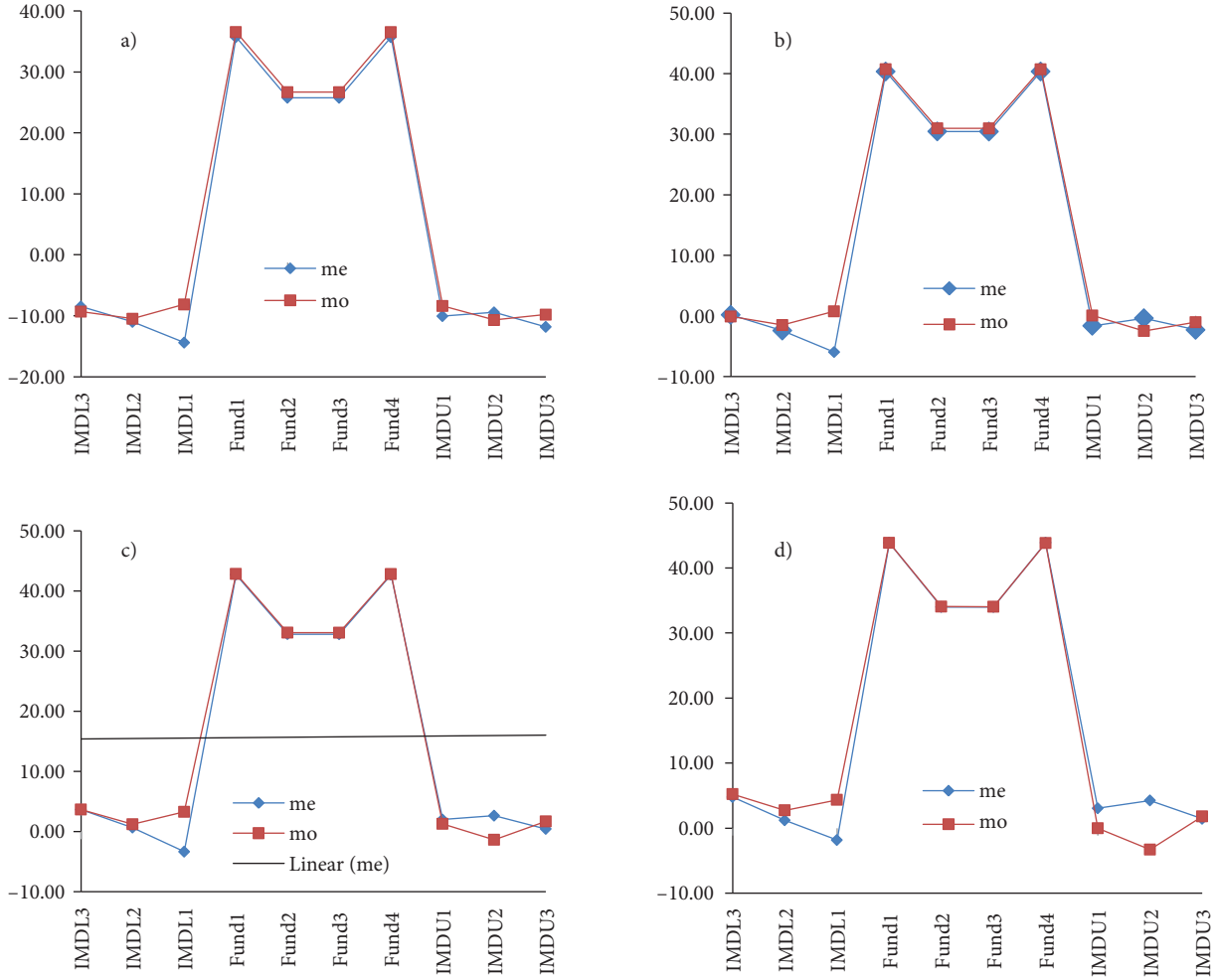

Figure 5. Comparison between the measurement and model outputs for a 4-tone (10-MHz/1-kHz) input excitation for: a) –7.8 dBm, b) –3.8 dBm, c) –1.8 dBm, and d) –0.8 dBm.

6. Conclusion

Although model parameters are found using 2-tone measurement results only, the model predictions and measurements are compared for various types of excitations.

It is demonstrated that using the introduced method behavior of a nonlinear amplifier can be represented successfully. This model incorporates time delay components that give an enhanced flexibility to the model, such that with a low-order polynomial a highly nonlinear system can be modeled. Not only the AM/AM but also AM/PM distortions are satisfactorily predicted, which indicates the proper consideration of the memory effects. The reason or source of these memory effects might be the nonlinearity of the semiconductor devices, thermal conditions, and low-frequency biasing circuits.

The explicit time delay terms permit examination of the relation of the memory terms to the operating conditions and the circuit components; consequently, the amplifiers can be designed accordingly. Moreover, these explicit relations can be utilized in linearization circuits, especially in DPD applications.

In this paper, a new behavioral model is proposed that is capable of characterizing asymmetric IMD behavior. The modeling approach is elaborated on an HF amplifier with a 45-dB gain and 100-W peak output

power. The response of the amplifier is measured both for 2-tone and 4-tone excitation input signals. These signals are created such that the center frequency is 10 MHz and the input power sweep range covers the power levels beyond P1 dB. Behavioral model parameters are extracted for this amplifier based on 2-tone measurement results using MATLAB's optimization tool.

References

[1] K. Remley, D. Williams, D. Schreurs, J. Wood, "Simplifying and interpreting two-tone measurements", IEEE Transactions on Microwave Theory and Techniques, Vol. 52, pp. 2576–2584, 2004.

[2] A. Saleh, "Frequency-independent and frequency-dependent nonlinear models of TWT amplifiers", IEEE Transactions on Communications, Vol. 29, pp. 1715–1720, 1981.

[3] K.Y. Huang, L. Yiming, L. Chien-Ping, "A time-domain approach to simulation and characterization of RF HBT two-tone intermodulation distortion", IEEE Transactions on Microwave Theory and Techniques, Vol. 51, pp. 2055–2062, 2003.

[4] P. Arno, F. Launay, J. Fournier, J. Grasset, "A simple RF power amplifier characterization using AM-AM, AM-PM measurements based on CDMA signal statistics", 34th European Microwave Conference, pp. 693–696, 2004.

[5] W. Ciccognani, P. Colantonio, F. Giannini, E. Limiti, M. Rossi, "AM/AM and AM/PM power amplifier characterisation technique", 15th International Conference on Microwaves, Radar and Wireless Communications, Vol. 2, pp. 678–681, 2004.

[6] J.T. Stonick, V.L. Stonick, J.M.F. Moura, R.S. Zborowski, "Memoryless polynomial adaptive predistortion [TV transmitters]", International Conference on Acoustics, Speech, and Signal Processing, Vol. 2, pp. 981–984, 1995.

[7] M. Faulkner, M. Johansson, "Adaptive linearization using predistortion-experimental results", IEEE Transactions on Vehicular Technology, Vol. 43, pp. 323–332, 1994.

[8] S. Boumaiza, F.M. Ghannouchi, "Realistic power-amplifiers characterization with application to baseband digital predistortion for 3G base stations", IEEE Transactions on Microwave Theory and Techniques, Vol. 50, pp. 3016–3021, 2002.

[9] N.B. Carvalho, J.C. Pedro, "Two-tone IMD asymmetry in microwave power amplifiers", IEEE MTT-S International Microwave Symposium Digest, Vol. 1, pp. 445–448, 2000.

[10] F.M. Ghannouchi, F. Taringou, O. Hammi, "A dual branch Hammerstein-Wiener architecture for behavior modeling of wideband RF transmitters", IEEE MTT-S International Microwave Symposium Digest, pp. 1692–1695, 2010.

[11] A. Bolstad, B.A. Miller, J. Goodman, J. Vian, J. Kalyanam,, "Identification and compensation of Wiener-Hammerstein systems with feedback", IEEE International Conference on Acoustics, Speech and Signal Processing, pp. 4056–4059, 2011.

[12] M. Masood, J. Wood, J. Staudinger, J.S. Kenney, "Behavioral modeling of high power RF amplifiers using pruned Volterra scheme with IIR basis functions", IEEE Topical Conference on Power Amplifiers for Wireless and Radio Applications, pp. 97–100, 2012.

[13] L. Guan, A. Zhu, "Simplified dynamic deviation reduction-based Volterra model for Doherty power amplifiers", Workshop on Integrated Nonlinear Microwave and Millimetre-Wave Circuits, pp. 1–4, 2011.

[14] Z. Huang, W. Chen, Z. Feng, F. M. Ghannouchi, "Forward behavioral modeling of concurrent dual-band power amplifiers using extended real valued time delay neural networks", International Conference on Microwave and Millimeter Wave Technology, Vol. 5, pp. 1–4, 2012.

[15] W. Huadong, B. Jingfu, W. Zhengdu, "Comparison of the behavioral modelings for RF power amplifier with memory effects", IEEE Microwave and Wireless Components Letters, Vol. 19, pp. 179–181, 2009.

[16] M. Isaksson, D. Wisell, D. Ronnow, "A comparative analysis of behavioral models for RF power amplifiers", IEEE Transactions on Microwave Theory and Techniques, Vol. 54, pp. 348–359, 2006.

[17] A.S. Tehrani, C. Haiying, S. Afsardoost, T. Eriksson, M. Isaksson, C. Fager, "A comparative analysis of the complexity/accuracy tradeoff in power amplifier behavioral models", IEEE Transactions on Microwave Theory and Techniques, Vol. 58, pp. 1510–1520, 2010.

[18] J.C. Pedro, S.A. Maas, "A comparative overview of microwave and wireless power-amplifier behavioral modeling approaches", IEEE Transactions on Microwave Theory and Techniques, Vol. 53, pp. 1150–1163, 2005.

[19] N.B. Carvalho, J.C. Pedro, "A comprehensive explanation of distortion sideband asymmetries", IEEE Transactions on Microwave Theory and Techniques, Vol. 50, pp. 2090–2101, 2002.

[20] J. Vuolevi, T. Rahkonen, J. Manninen, "Measurement technique for characterizing memory effects in RF poweramplifiers", IEEE Transactions on Microwave Theory and Techniques, Vol. 49, pp. 1383–1389, 2001.

[21] K. Hyunchul, M.D. McKinley, J.S. Kenney, "Extraction of accurate behavioral models for power amplifiers with memory effects using two-tone measurements", IEEE MTT-S International Microwave Symposium Digest, pp. 139–142, 2002.

[22] W. Jang, A. Walker, K. Gard, M. Steer, "Capturing asymmetrical spectral regrowth in RF systems using a multislice behavioral model and enhanced envelop transient analysis", International Journal of RF and Microwave Computer Aided Engineering, Vol. 16, pp. 400, 2006.

[23] A.H. Yuzer, S. Demir, "A new phase measurement technique for RF power amplifier only measuring magnitudes", Progress in Electromagnetics Research Symposium, 2010.

[24] A.H. Yuzer, "Modeling of asymmetric intermodulation distortion and memory effects of power amplifiers", PhD Thesis, University of Middle East Technical University, Ankara, Turkey, 2011.

[25] A. Haider, A. Chatterjee, "Low-cost alternate EVM test for wireless receiver systems", Proceedings of the 23rd IEEE VLSI Test Symposium, pp. 255–260, 2005.